Journal of Power Sources 196 (2011) 5867–5872

Contents lists available at ScienceDirect

Journal of Power Sources

journal homepage: www.elsevier.com/locate/jpowsour

Fuel cell/battery passive hybrid power source for electric powertrains

Jérôme Bernard[a,*], Marcel Hofer[a], Uwe Hannesen[b], Antoine Toth[c], Akinori Tsukada[a], Félix N. Büchi[a,**], Philipp Dietrich[a]

[a] Electrochemistry Laboratory, Paul Scherrer Institut, 5232 Villigen-PSI, Switzerland
[b] Belenos Clean Power Holding SA, Rue des Sors 3, 2074 Marin, Switzerland
[c] Swatch Group, C/O Micro Crystal EBOSA, Kapellestrasse 30, 2540 Grenchen, Switzerland

ARTICLE INFO

Article history:
Received 26 November 2010
Received in revised form 14 February 2011
Accepted 8 March 2011
Available online 15 March 2011

Keywords:
Fuel cell
Battery
Powertrain
Hybrid

ABSTRACT

The concept of passive hybrid, i.e. the direct electrical coupling between a fuel cell system and a battery without using a power converter, is presented as a feasible solution for powertrain applications. As there are no DC/DC converters, the passive hybrid is a cheap and simple solution and the power losses in the electronic hardware are eliminated. In such a powertrain topology where the two devices always have the same voltage, the active power sharing between the two energy sources can not be done in the conventional way. As an alternative, control of the fuel cell power by adjusting its operating pressure is elaborated. Only pure H_2/O_2 fuel cell systems are considered in this approach. Simulation and hardware in the loop (HIL) results for the powertrain show that this hybrid power source is able to satisfy the power demand of an electric vehicle while sustaining the battery state of charge.

1. Introduction

In a fuel cell hybrid vehicle, the electric propulsion motor(s) is powered by a fuel cell system coupled to a battery. A polymer electrolyte fuel cell (PEFC) [1–3] converts hydrogen and oxygen into electrical power with only water and heat as the byproducts. The battery is used as an energy buffer [4,5]: it power assists the fuel cell system during peak power demands (vehicle acceleration), recovers partially the kinetic energy of the vehicle during braking phases, and allows shifting to a certain degree the fuel cell operating point for optimizing the efficiency. Generally, the battery is used in a charge sustaining mode, i.e. the state of charge evolutes around a prescribed value and no external charger is used.

There are two categories of fuel cell hybrid power sources: active and passive hybrids [6] (Fig. 1). In an active hybrid architecture (Fig. 1a), there is at least one DC/DC converter between the fuel cell and the battery. The DC/DC converter(s) adapts the voltage of each device to the bus voltage and permits to actively control the power sharing between each source. A power management strategy is needed to determine this power sharing according to a certain objective (for example the fuel consumption) while respecting constraints (battery state of charge limits, power limits, etc.) [7–9].

In a passive hybrid architecture (Fig. 1b), the fuel cell and the battery are directly connected to the bus without DC/DC converter(s). Only a switch may be present to connect or disconnect the fuel cell from the bus. As long as the switch is closed, the two components operate at the same voltage [10]. This causes disadvantages [11–13]: (1) the sizing is highly constrained because the voltages deviations of the sources have to match, (2) such an architecture reduces the overall specific power of the hybrid power source as highlighted in Figs. 2 and 3) the bus voltage and the currents regulate themselves according to the impedance of the fuel cell system and the battery. This last point reveals that the system variables (currents, voltage, powers, state of charge) are uncontrolled (no power management strategy is possible) and can therefore reach or exceed their limits, leading eventually to system breakdown.

Therefore the active hybrid has been established as the preferred topology since it has less constraints in comparison to the passive hybrid topology. However, as there are no DC/DC converters, the passive hybrid is the cheaper and the simpler solution, and the power losses in the electronic hardware are eliminated. This paper, addressing only fuel cell systems operated with pure oxygen, shows that also a passive hybrid can become a suitable solution for powertrain applications when the power sharing becomes actively controlled. One solution to achieve an active power sharing is to vary the internal impedance of the fuel cell by controlling its operating pressure.

In the first part of this paper, the characteristics of the hydrogen/oxygen fuel cell system are presented. Then in the next section the concept of the passive hybrid is exposed in details. Section 4

* Corresponding author. Tel.: +41 56 310 55 88; fax: +41 56 310 21 99.
** Corresponding author. Tel.: +41 56 310 24 11.
E-mail addresses: jerome.bernard@psi.ch (J. Bernard), felix.buechi@psi.ch (F.N. Büchi).

0378-7753/$ – see front matter © 2011 Elsevier B.V. All rights reserved.
doi:10.1016/j.jpowsour.2011.03.015

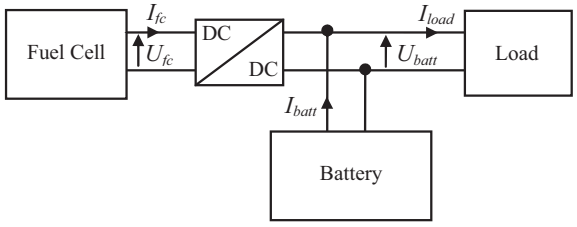

a Active hybrid with DC/DC converter between the FC and the battery.

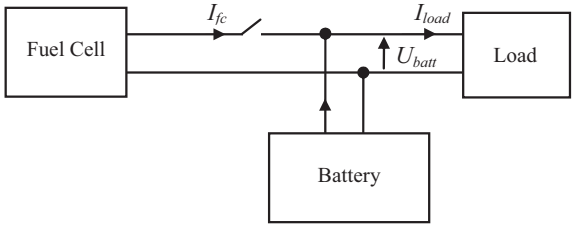

b Passive hybrid with direct connection between the FC and the battery.

Fig. 1. Passive (a) and active (b) FC/battery hybrid powertrain architectures.

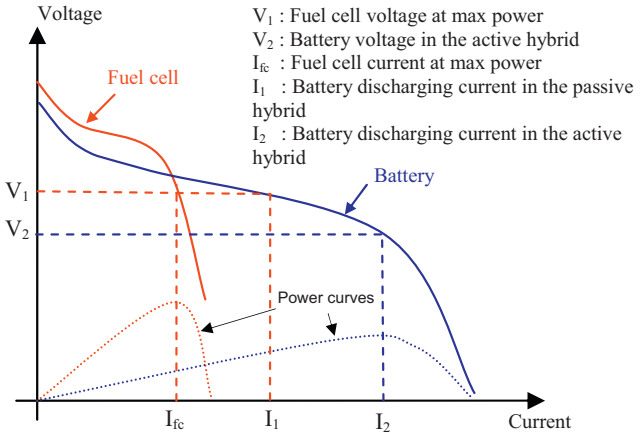

Fig. 2. Passive and active maximum power [13]. The voltage–current curves of the fuel cell and the battery show that the output power in the active hybrid is higher than in the passive hybrid.

provides simulation results of a vehicle under different driving conditions. The last part of the paper discusses the advantages and the drawbacks of the passive hybrid solution.

2. Fuel cell system

The fuel cell system considered is a H_2/O_2 PEFC system. Such a system using pure oxygen as the oxidant is not commonly used for powertrain applications where the H_2/air fuel cell systems are dominating. A H_2/O_2 PEFC system brings yet several advantages such as higher specific power, higher efficiency, higher system dynamics and easier water management [14]. The main disadvantages are the need of oxygen production and it's on board storage, but this can be balanced by the higher efficiencies achieved by such powertrains [15].

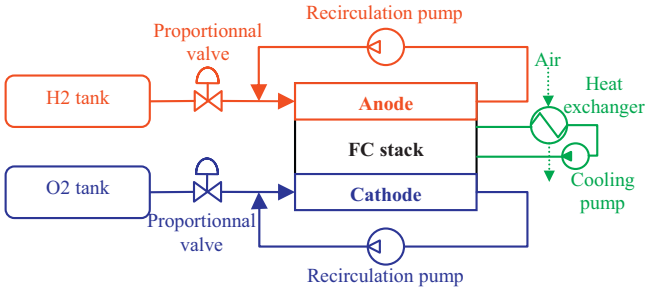

Fig. 3. Simplified scheme of a H_2/O_2 fuel cell system.

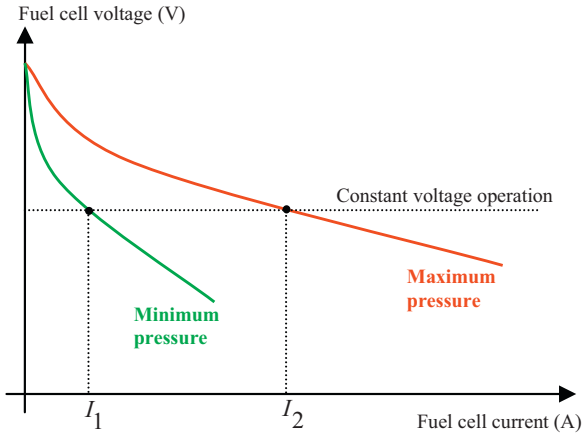

Fig. 4. Example of polarization curves of a fuel cell stack at different operating pressures.

Fig. 3 shows a simplified scheme of a H_2/O_2 PEFC system. It is composed from a PEFC stack surrounded by auxiliary components. The auxiliaries are grouped into three main circuits (Fig. 3): (1) the hydrogen circuit on the anode side, (2) the oxygen circuit on the cathode side and (3) the cooling circuit. The cathode and anode pressures are controlled by means of proportional valves. The hydrogen and oxygen gases are re-circulated from stack outlet to stack inlet by means of recirculation pumps. The recirculation loops contain also water separators and purge valves which are not shown in Fig. 3.

The electrical characteristics of a fuel cell are described by its polarization curve (Fig. 4). This polarization curve is pressure and temperature dependent. For instance, at a constant temperature and a constant voltage, the fuel cell current decreases when decreasing the gas pressures (Fig. 4). For example, at a given voltage, the fuel cell current is minimal at the lowest pressure (Fig. 4, current I_1) and reaches it's maximum at the highest operating pressure (Fig. 4, current I_2).

Further experimental result is shown in Fig. 5. This measurement was performed with a 10 kW fuel cell stack operated in a

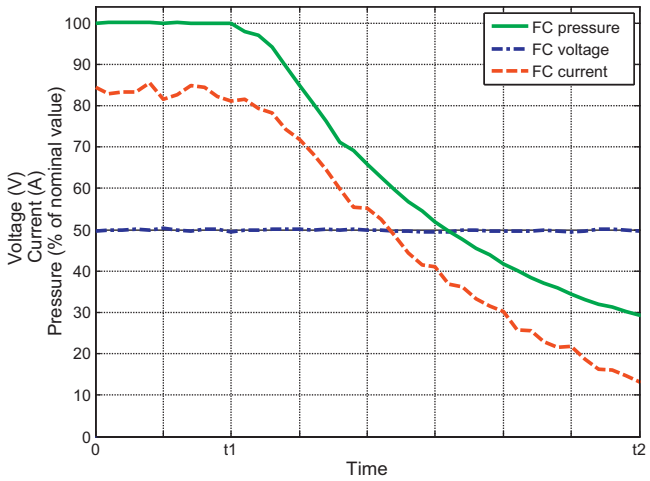

Fig. 5. Current and pressure variation of a PEFC stack operated at constant voltage.

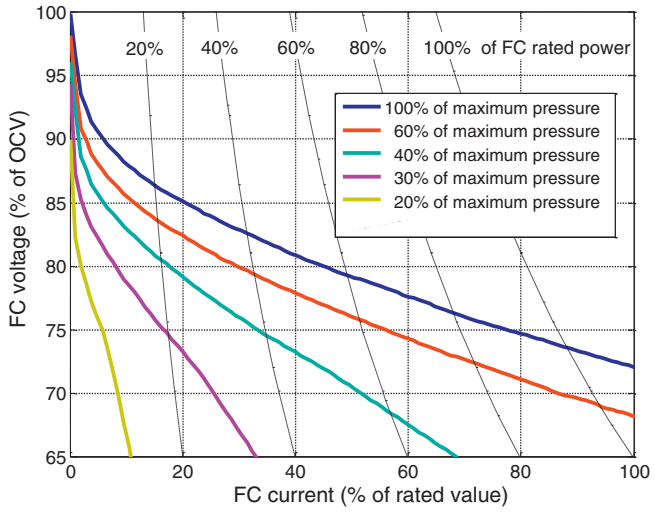

Fig. 6. Polarization curves at nominal temperature and different pressures.

laboratory testbench. The load connected to the FC stack operated at a constant voltage of 50 V. Until $t = t_1$, the FC pressure (cathode and anode pressures) is nominal and the corresponding current is 85 A. Then between $t = t_1$ and $t = t_2$, the FC pressure is reduced from 100% to 30% of nominal value, which concomitantly decreases the FC current from 85 A to near 13 A.

Considering the results from Figs. 4 and 5, it means that in the case of a passive hybrid where the battery imposes its voltage to the fuel cell, the fuel cell current can be adjusted by controlling the pressure. The next sections investigate in more detail the feasibility of this concept for powertrain applications.

3. Passive hybrid concept

3.1. Fuel cell model

In a first approach, a steady state model of the fuel cell system is considered [1]. The model uses real experimental data to simulate a full scale stack; Fig. 6 shows the polarization curves measured at nominal temperature for different operating pressures; the dashed lines represent the stack power and they are expressed as a percentage of rated power P_{max}. The minimum voltage allowed is 70% of the open circuit voltage (OCV) and the maximum voltage is 85% of OCV to limit degradations. The parasitic load for the H_2/O_2 system (auxiliary components consumption) is considered constant at 2% of the FC maximum power.

A pressure variation rate is also considered in the model. In a H_2/O_2 fuel cell system, the pressures at the anode and cathode can increase quickly (positive rate higher than 0.5 bar s^{-1}). This fast positive rate is constrained by the dynamic of the proportional valves and by their orifices sections (defining the maximum gas flow). Pressure reductions are achieved by closing the proportional valves (Fig. 3) while drawing a fuel cell current. Assuming than the anode and the cathode have similar volumes, the negative rate is constrained by the oxygen consumption only. This negative rate can be estimated according to the FC current and the cathode parameters (when water vapor is neglected):

$$\dot{p}_{O_2}(t) = \frac{\dot{n}_{O_2}(t) \cdot R \cdot T_{fc}(t)}{V_{cathode}} \quad (1)$$

with

$$\dot{n}_{O_2}(t) = \frac{I_{fc}(t)}{4 \cdot F} \cdot N_{cell} \quad (2)$$

Table 1
Battery parameters.

Cell type	3.6 V SAFT VL34P
Nominal voltage	3.6 V $cell^{-1}$
Nominal capacity	33 Ah
Internal resistance	1 mΩ $cell^{-1}$
Faradic efficiency	99%
Peak discharge current	15 C
Maximum voltage	4.1 V $cell^{-1}$
Minimum voltage	2.0 V $cell^{-1}$

with $\dot{p}_{O_2}$ the pressure decrease rate (Pa s^{-1}), $\dot{n}_{O_2}$ the oxygen consumption rate (mol s^{-1}), R the ideal gas constant (m^2 kg s^{-2} K^{-1} mol^{-1}), $T_{fc}(t)$ the fuel cell mean temperature (K), $V_{cathode}$ the total volume of the cathode gas circuit (m^3), I_{fc} the stack current (A), N_{cell} the number of cells in the stack and F the Faraday number (C). With a volume of 5 l of the cathode gas circuit, a 200 cell stack operating at 80 °C and a current of 50 A, a decrease rate of the fuel cell pressure of 0.15 bar s^{-1} is achieved.

The achievable increasing and decreasing pressure rates allow for sufficient dynamics of the fuel cell power for the automotive powertrain application.

3.2. Battery model

The equivalent circuit model used for the battery is composed from a voltage source in series with a resistor [16,17]. The open circuit voltage OCV_{batt} and the resistor R_{batt} are function of the state of charge (SOC), which is calculated by current integration:

$$C_{batt}(t) = C_{batt}(0) - \frac{1}{3600} \int_0^t \eta_f(SOC(u), sign(I_{batt}(u)) \cdot I_{batt}(u) \cdot du \quad (3)$$

$$SOC(t) = \frac{C_{batt}(t)}{\overline{C_{batt}}} \quad (4)$$

with C_{batt} is the battery capacity (Ah), $\overline{C_{batt}}$ is the nominal capacity (Ah), η_f is the faradic efficiency (–) and I_{batt} the battery current (A).

The battery voltage U_{batt} depends on the state of charge SOC and on the current I_{batt}:

$$U_{batt}(SOC, I_{batt}) = OCV_{batt}(SOC) - R_{batt}(SOC, sign(I_{batt})) \cdot I_{batt} \quad (5)$$

with

$$R_{batt}(SOC, sign(I_{batt})) = \begin{cases} R_{charge}(SOC) & \text{if } I_{batt} \leq 0 \quad \text{(charge)} \\ R_{discharge}(SOC) & \text{if } I_{batt} > 0 \quad \text{(discharge)} \end{cases} \quad (6)$$

3.3. Passive hybrid power source

Considering the passive hybrid architecture, the fuel cell and battery models are linked by their voltage, $U_{fc}(t) = U_{batt}(t)$ (Fig. 1b). Considering this constraint, it is possible to deduce (1) the power available at the bus for the electric traction and (2) the influence of the fuel cell operating pressure on the power sharing.

The battery used for the simulation is a based on Li-ion cells with the parameters specified in Table 1. The battery has been sized (number of cells in series) to match the fuel cell system operating voltage range described in Section 3.1 and shown in Fig. 6.

Fig. 7 shows the power available from the fuel cell and the battery. The red lines refer to the fuel cell: the two bold red lines represent the polarization curves at maximum and minimum pressure, and the thin red lines represent the FC iso-power curves (expressed in percentage of maximum power). The blue color refers to the battery: the bold blue lines indicate the voltages limits of the battery (at 100% maximum discharge power and 50% maximum charge power), the thin line indicates the iso-power lines (expressed in percentage of maximum power), and the blue dashed line represents the battery OCV at 50% state of charge. Using Fig. 7, the

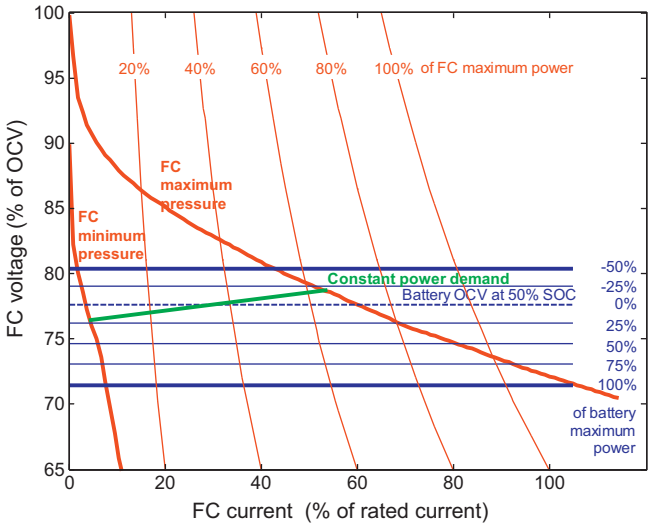

Fig. 7. Power available from the fuel cell and the battery in the passive hybrid architecture.

power available at the bus is achieved easily by summing the fuel cell power and the battery power. The fuel cell polarization curves limits are temperature dependent. The battery limits of operation, represented by blue bold lines in Fig. 7, are temperature and state of charge dependent: if the state of charge increases (respectively decreases), the battery OCV and voltage operation area shift up (respectively down).

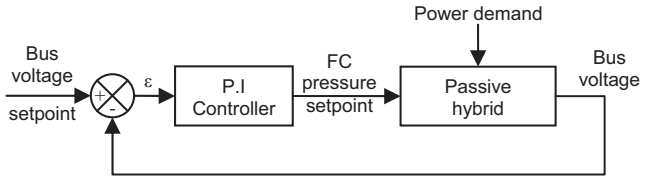

Fig. 8. FC pressure controller in passive hybrid powertrain.

The green segment Fig. 7 represents a constant positive power demand from the bus. This segment is delimited by the upper and lower fuel cell polarization curve (corresponding, respectively, to the maximum and minimum fuel cell pressures). By adjusting the pressure, and for the same bus power demand, it is possible to move the operating point along this segment and thus control the power sharing between the fuel cell and the battery. For instance, according to the green segment in Fig. 7, at maximum pressure the fuel cell provides 65% of its rated power and the battery provides −18% of its rated power (charge); for the same bus power demand, at minimum pressure the fuel cell provides 5% of its rated power and the battery provides 20% of its rated power (discharge); at an intermediate pressure, where the battery power is zero, the fuel cell satisfies the load alone with 33% of its rated power.

4. Powertrain simulation

4.1. Powertrain parameters

The passive hybrid power source described in the previous section is considered to supply the electric powertrain of a light

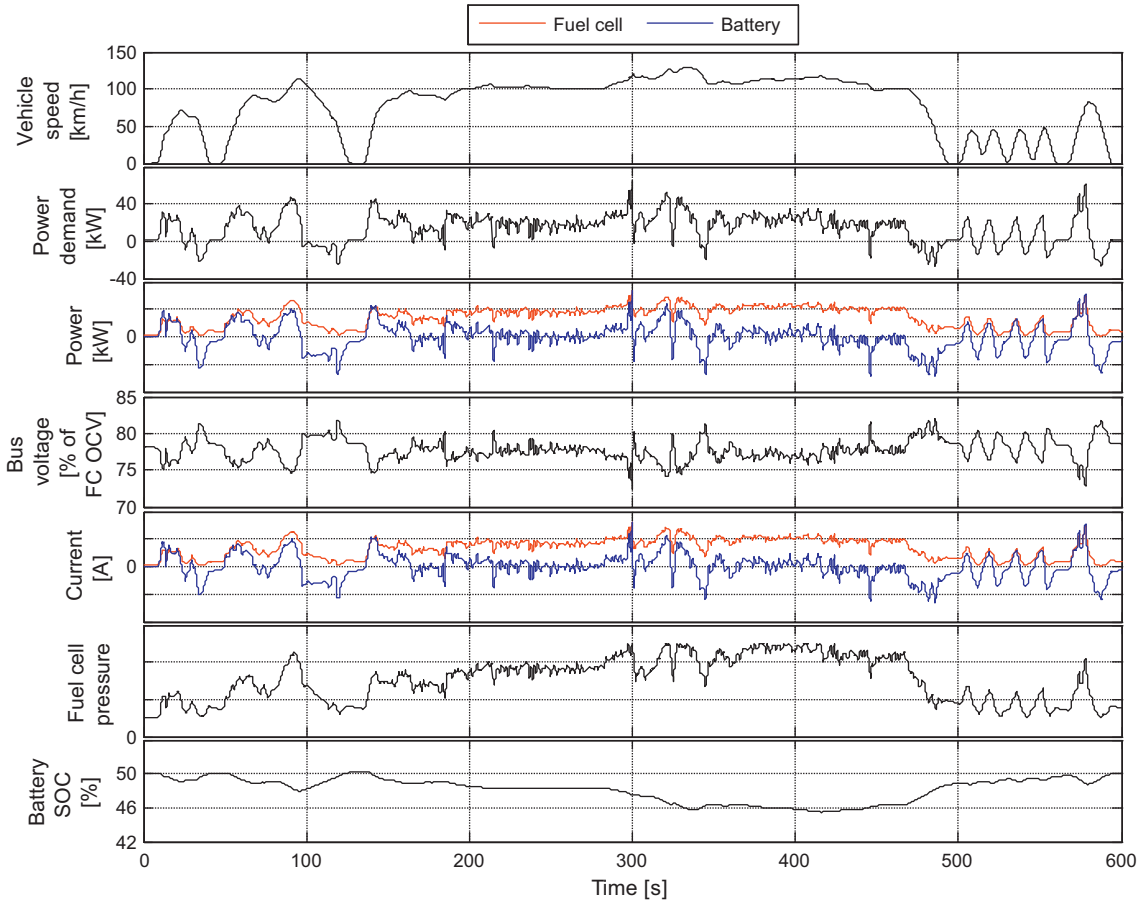

Fig. 9. Simulation results of the passive hybrid powertrain for the US06 driving cycle.

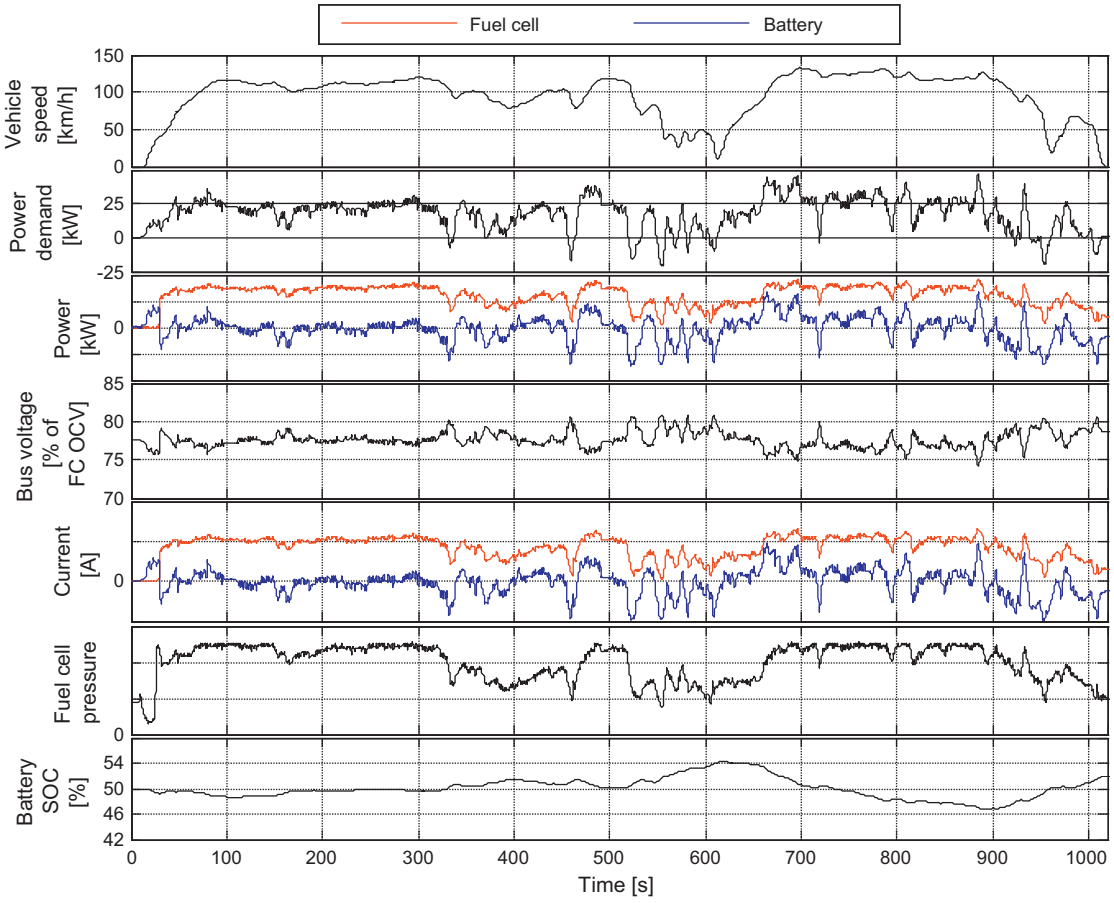

Fig. 10. HIL experiment of the passive hybrid powertrain for a highway driving cycle.

passenger car. The power demand is calculated with an energetic model of a car driving a defined speed cycle. This power demand is increased by the consumption of the fuel cell auxiliaries. The parameters of the vehicle are provided in Table 2.

4.2. Power management strategy

The power management strategy defines the power sharing between the fuel cell and the battery. This sharing calculation is defined according to an objective function (for example the minimization of the fuel consumption) and respects system constraints (for instance voltage limitations). This power sharing is possible with the use of a control variable. In the present case, the control variable is the fuel cell operating pressure.

In the passive hybrid architecture, the fuel cell and the battery operate at the same voltage. It is important that this voltage remains within the operating voltage range of both devices to avoid degradation or failures. Therefore, it is chosen to regulate the bus voltage around a prescribed setpoint. Ideally, this setpoint corresponds to the nominal battery voltage, which ensures that state of charge stays around its nominal value. A controller adjusts the fuel cell operating pressure according to the bus voltage variation. The control loop is resumed in Fig. 8. The bus voltage setpoint corresponds to battery OCV at 50% state of charge.

Table 2
Vehicle parameters of light passenger car used for the model.

Mass	1000 kg
Aerodynamic drag coefficient	0.35
Frontal area	1.9 m^2
Rolling resistance	0.009
Motor peak power	120 kW
Motor continuous power	60 kW
Motor average efficiency	80%
Motor peak efficiency	95%
Motor DC/AC efficiency	95%
Motor DC/AC constant power consumption	300 W

4.3. Simulation results

Simulation results are given Fig. 9 for the US06 driving cycle. The US06 cycle with an average speed of 77 km h^{-1} tests the controllability of the powertrain for high average bus power requirements. The results show that the power demand of the powertrain can be satisfied by the fuel cell passive hybrid power source. The fuel cell pressure controls the bus voltage which makes the battery state of charge evolving around 50%. The bus voltage variation remains within the fuel cell voltage range specified (between 70% and 85% OCV).

For more validating the feasibility of the passive hybrid concept, hardware in the loop (HIL) experiments were performed [9]. This method consists of replacing parts of the model in the simulation by real components. Here, the fuel cell model is replaced by a real fuel cell system operating in a laboratory bench. The real fuel cell is voltage controlled while the voltage and fuel cell pressure setpoint are computed by the model. Finally, the measured fuel cell current is transferred to the model to close the simulation loop. These experiments intend to reproduce real operating conditions of a fuel cell system that would operate in a passive hybrid powertrain. A result of these experiments is given in Fig. 10 for the A2 highway driving condition [18]. It is shown in Fig. 10 that the fuel cell is able

to adjust its power by varying the pressure. This allows, as observed in the simulation in Fig. 9, to control the bus voltage which remains between 75% and 82% of fuel cell OCV. The HIL experiments prove that the fuel cell system can successfully be operated under the conditions imposed by a passive hybrid architecture.

5. Advantages and drawbacks

Based on component measurements and a model, it has been shown that a fuel cell passive hybrid power source based on a H_2/O_2 fuel cell system (using pure oxygen) is able to fulfill the power demand of a powertrain while sustaining the state of charge of the battery under most driving conditions (average power less than fuel cell rated power) and keeping voltage and current within reasonable limits. However, still the passive hybrid configuration needs some considerations.

First, the fuel cell system is forced to operate at pressures lower than its nominal value which reduces its efficiency. This however is at least balanced by the absence of DC/DC converter losses. Preliminary calculations showed that the fuel consumption of a fuel cell passive hybrid powertrain is not higher than the one of an active hybrid. The global efficiency is even higher when driving on the highway because the high power and high energy demands forces the fuel cell to operate at its nominal pressure, so its nominal efficiency, without losses in a DC/DC converter.

Second, when operating the fuel cell with pressures below 1 bar absolute, the anode and the cathode gas compartments cannot be purged to the ambient otherwise air would be sucked into the circuits. These purges are necessary to remove inert gases accumulating in the stack due to impurities of feed gases, and they are also needed to drain the water separators especially at the cathode side where water is produced. It becomes obvious that low pressure operation can therefore not be maintained infinitely. A possible solution is to increase temporarily the pressure above ambient to enable the purges. Realizing pressures below ambient is less straight forward for conventional H_2/air fuel cell systems, and therefore considerably reduces the possibilities of the passive hybrid architecture in this case, even if it has also been proposed for power train application [19].

At last, since the fuel cell and the battery voltages are equal, the sizing of each of the devices needs to be considered carefully. The degree of freedom in sizing is considerably reduced as compared to the active hybrid architecture [20] where the DC/DC converter adapts the voltages to the bus voltage. The battery voltage operating range is defined by its maximum voltage in charge and its minimum voltage in discharge. This range must fit into the fuel cell voltage operating range to avoid permanent degradation of one or the other device.

6. Conclusion

This paper shows that with a H_2/O_2 fuel cell system (using pure oxygen) an active power sharing can be realized in a fuel cell/battery passive hybrid power source by adjusting the fuel cell operating pressure. This allows for sustaining the battery state of charge and to fulfill the power demand of an automotive powertrain. The absence of a DC/DC converter connected to the fuel cell or the battery makes the system easier, lighter and cheaper. However, it is important to define the correct battery and fuel cell parameters in order that both devices operate in a matched voltage range.

This study is a preliminary analysis of fuel cell passive hybrid powertrains. Next investigations should concentrate on efficiency issues. Especially, both passive and active hybrid architectures have to be carefully compared to define the best solution according to driving conditions and vehicle specifications.

Acknowledgment

The present research work has been supported by the Belenos Clean Power Holding. The authors gratefully acknowledge the support.

References

[1] D.D. Boettner, G. Paganelli, Y.G. Guezennec, G. Rizzoni, M.J. Moran, J. Energy Res. Technol. 124 (2002) 20–27.
[2] P. Dietrich, F.N. Büchi, A. Tsukada, M. Bärtschi, R. Kötz, G.G. Scherer, P. Rodatz, O. Garcia, M. Ruge, M. Wollenberg, P. Lück, A. Wiartalla, C. Schönfelder, A. Schneuwly, P. Barrade, Handb. Fuel Cells: Fundam. Technol. Appl. 4 (2003) 1184–1198.
[3] Emadi, K. Rajashekara, S. Williamson, S. Lukic, IEEE Trans. Vehicle Technol. 54 (2005) 763–770.
[4] T. Markel, M. Zolot, K.B. Wipke, A.A. Pesaram, Advanced Automotive Battery Conference, 2003.
[5] K.S. Jeong, B.S. Oh, J. Power Sources 105 (2002) 58–65.
[6] R. Saïsset, C. Turpin, S. Astier, J.M. Blaquière, IEEE Vehicle Power and Propulsion Conference, 2004.
[7] J. Bernard, S. Delprat, F.N. Büchi, T.M. Guerra, Int. Rev. Elect. Eng. 1 (2006) 352–362.
[8] L. Sciarretta, Guzzella, IEEE Control Syst. Mag. 27 (2007) 60–70.
[9] J. Bernard, S. Delprat, T.M. Guerra, F.N. Büchi, Control Eng. Pract. 18 (2010) 408–417.
[10] M.J. Blackwelder, R.A. Dougal, J. Power Sources 134 (2004) 139–147.
[11] Z. Jiang, L. Gao, M. Blackwelder, R.A. Dougal, J. Power Sources 71 (2004) 130–163.
[12] L. Gao, Z. Jiang, R.A. Dougal, IEEE Trans. Aerosp. Electron. Syst. 41 (2005) 346–355.
[13] Z. Jiang, R.A. Dougal, IEEE Trans. Ind. Electron. 53 (2006) 1094–1104.
[14] F.N. Büchi, S.A. Freunberger, M. Reum, G. Paganelli, A. Tsukada, P. Dietrich, A. Delfino, Fuel Cells 7 (2007) 159–164.
[15] F.N. Büchi, G. Paganelli, P. Dietrich, D. Laurent, A. Tsukada, P. Varenne, A. Delfino, R. Kötz, S.A. Freunberger, P.A. Magne, D. Walser, D. Olsommer, Fuel Cells 7 (2007) 329–335.
[16] V.H. Johnson, J. Power Sources 110 (2002) 321–329.
[17] J. Van Mierlo, P. Van den Bossche, G. Maggetto, J. Power Sources 128 (2004) 76–89.
[18] M. André, R. Joumard, R. Vidona, P. Tassela, P. Perret, Atmos. Environ. 40 (2006) 5944–5953.
[19] T.M. Keranen, H. Karimaki, J. Viitakangas, J. Vallet, J. Ihonen, P. Hyotyla, H.Uusalo, T. Tingelof, J. Power Sources (2011), doi:10.1016/j.jpowsour.2011.01.025.
[20] J. Bernard, S. Delprat, F.N. Büchi, T.M. Guerra, IEEE Trans. Vehicle Technol. 58 (2009) 3168–3176.